Characterization of a thiamin diphosphate-dependent phenylpyruvate decarboxylase from *Saccharomyces cerevisiae*

Malea M. Kneen[1], Razvan Stan[1], Alejandra Yep[2], Ryan P. Tyler[2], Choedchai Saehuan[2,*] and Michael J. McLeish[1]

1 Department of Chemistry and Chemical Biology, Indiana University-Purdue University Indianapolis, IN, USA
2 Department of Medicinal Chemistry, University of Michigan, Ann Arbor, MI, USA

The product of the *ARO10* gene from *Saccharomyces cerevisiae* was initially identified as a thiamine diphosphate-dependent phenylpyruvate decarboxylase with a broad substrate specificity. It was suggested that the enzyme could be responsible for the catabolism of aromatic and branched-chain amino acids, as well as methionine. In the present study, we report the overexpression of the *ARO10* gene product in *Escherichia coli* and the first detailed *in vitro* characterization of this enzyme. The enzyme is shown to be an efficient aromatic 2-keto acid decarboxylase, consistent with it playing a major *in vivo* role in phenylalanine, tryptophan and possibly also tyrosine catabolism. However, its substrate spectrum suggests that it is unlikely to play any significant role in the catabolism of the branched-chain amino acids or of methionine. A homology model was used to identify residues likely to be involved in substrate specificity. Site-directed mutagenesis on those residues confirmed previous studies indicating that mutation of single residues is unlikely to produce the immediate conversion of an aromatic into an aliphatic 2-keto acid decarboxylase. In addition, the enzyme was compared with the phenylpyruvate decarboxylase from *Azospirillum brasilense* and the indolepyruvate decarboxylase from *Enterobacter cloacae*. We show that the properties of the two phenylpyruvate decarboxylases are similar in some respects yet quite different in others, and that the properties of both are distinct from those of the indolepyruvate decarboxylase. Finally, we demonstrate that it is unlikely that replacement of a glutamic acid by leucine leads to discrimination between phenylpyruvate and indolepyruvate, although, in this case, it did lead to unexpected allosteric activation.

Introduction

The Ehrlich pathway, which permits the use of leucine, isoleucine, valine, methionine, tyrosine, tryptophan or phenylalanine as a sole nitrogen source, leads to the formation of the fusel alcohols and acids (Fig. 1) [1]. Indeed, in *Saccharomyces cerevisiae*, the Ehrlich pathway is the only route for phenylalanine and

Abbreviations

BFDC, benzoylformate decarboxylase; IPDC, indole-3-pyruvate decarboxylase; IPyA, indole-3-pyruvic acid; KdcA, keto acid decarboxylase; PDB, Protein Data Bank; PDC, pyruvate decarboxylase; PPA, phenylpyruvic acid; PPDC, phenylpyruvate decarboxylase; ThDP, thiamin diphosphate.
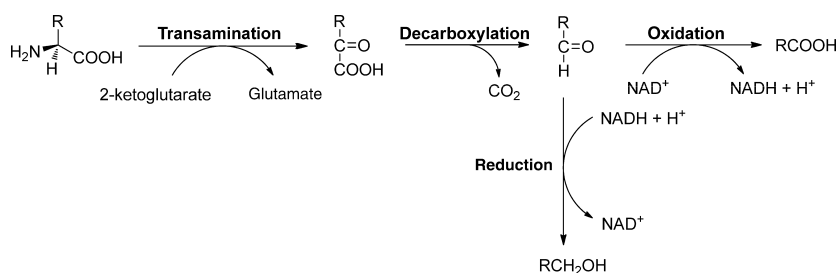
tryptophan catabolism [2]. The amino acids are initially transaminated to 2-keto acids and, in the subsequent irreversible step, the 2-keto acids are decarboxylated by any of several thiamin diphosphate (ThDP)-dependent decarboxylases. Depending on the redox state of the cell [3], the resulting aldehydes are then converted by a suite of alcohol and aldehyde dehydrogenases to fusel alcohols or acids, respectively [4]. The fusel products are finally excreted into the surrounding medium. In yeast-fermented foods and beverages, these products are important contributors to flavors, both desirable and undesirable [1]. Recently, interest in this pathway has extended to a potential role in the production of biofuels. Branched-chain alcohols have significant advantages, such as higher energy density and lower hygroscopicity, over ethanol [5]. Consequently, there is considerable attention being paid to those enzymes that are involved in the production of branched-chain 2-keto acids [5,6].

S. cerevisiae expresses several ThDP-dependent decarboxylases that permit the assimilation of the aromatic and branched-chain amino acids [7–9]. The three pyruvate decarboxylase (PDC) isoforms, PDC1 [10], PDC5 [11] and PDC6 [12], are the best-studied of these enzymes. The presence of PDC-independent decarboxylase activity in *S. cerevisiae* was suggested by the ability of PDC-deletion strains to metabolize both branched-chain and aromatic amino acids [8]. This ability was traced to the *ARO10* gene, also known as YDR380w, which was induced by tryptophan through the same mechanism as *ARO9*, the gene encoding aromatic aminotransferase II [13]. The latter enzyme catalyzes the first step in aromatic amino acid catabolism and is induced by aromatic amino acids via the transcription factor Aro80 [13]. Subsequently, *ARO10* was found to be inducible by growth on phenylalanine as a sole nitrogen source, and it was shown that the *ARO10* gene product, *Sc*PPDC, was a phenylpyruvate decarboxylase with a broad substrate specificity [4]. In addition to being upregulated by methionine and leucine [4], transcriptome analyses of *S. cerevisiae* cells grown on various nitrogen sources showed that isoleucine and threonine also trigger transcription of Aro80

target genes [14]. Therefore, potentially, *ARO10* and its associated genes may be responsible for the catabolism of aromatic and branched-chain amino acids, as well as methionine. However, *Sc*PPDC is essentially unable to utilize pyruvate [4].

As part of an ongoing project in our laboratory, we are interested in determining the rules that govern substrate specificity in ThDP-dependent decarboxylases. In the first instance, we focused on converting benzoylformate decarboxylase (BFDC) into a PDC, which involved shifting the enzyme's preference from binding a phenyl group to binding a methyl group [15,16]. Although the results obtained from those studies have been promising, with a 11 000-fold improvement in pyruvate utilization by BFDC [16], the experimental design has been complicated by differences in the position of the catalytic residues in the two decarboxylases [17]. *Sc*PPDC is more similar to *S. cerevisiae* PDC1 (32% identity, 45% similarity) than is BFDC (18% identity, 33% similarity), and it was considered that *Sc*PPDC may prove to be a more tractable subject for conversion to a PDC. *Sc*PPDC may also be considered an attractive target for manipulation of the production of fusel alcohols for the food, cosmetics and biofuel industries [1], as well as being useful for stereospecific carboligation reactions [18].

In the present study, we report the overexpression of the *ARO10* gene product in *Escherichia coli* and the first detailed *in vitro* characterization of this enzyme (UniProt ID: Q06408). The initial steps towards understanding the factors influencing decarboxylation of shorter chain-length substrates are also reported. Finally, we test the proposal [19] that a single residue may be used to differentiate between the phenylpyruvate decarboxylases and the indolepyruvate decarboxylases (IPDCs).

Results and Discussion

The *ARO10* gene product has been identified as a phenylpyruvate decarboxylase with a broad spectrum of activity [3,4]. PPDCs have been reported in a range of bacterial species, including *Achromobacter eurydice*

[20], *Acinetobacter calcoaceticus* [21], *Pseudomonas putida* [22], *Nocardia* sp. 239 [23] and *Thauera aromatica* [23,24], although none of these enzymes has been characterized in detail. PPDC activity has also been observed in crude extracts of *Aspergillus niger* [25] and BLAST searches [26] indicate that PPDCs are likely to exist in other fungal species. Similar to the latter enzymes, at approximately 72 kDa, the *Sc*PPDC is predicted to be almost 20% larger than most ThDP-dependent decarboxylases. Nonetheless, the signature features of a ThDP-dependent enzyme are maintained.

In the present study, the gene encoding *Sc*PPDC was amplified from *S. cerevisiae* genomic DNA and visualized as an approximately 1.9 kb band on a 0.8% agarose gel. This corresponded with the expected size of the *ARO10* gene (http://db.yeastgenome.org) and sequencing of the PCR product confirmed the fidelity of the amplification. The gene product was expressed in *E. coli* as a C-terminal 6× His variant and was found primarily as soluble protein in the cell-free fraction. *Sc*PPDC-His was purified to homogeneity (Fig. 2) and remained stable for at least 6 months when kept at −80 °C in storage buffer. On the basis of SDS/PAGE chromatography, the apparent molecular mass of *Sc*PPDC-His was approximately 66 kDa (Fig. 2). This was at odds with the calculated molecular mass of 72.3 kDa determined from the translated amino acid sequence. However, the *Sc*PPDC sample was clearly larger than an authentic sample of BFDC

from *P. putida* (57.4 kDa) when run on the same gel (Fig. 2). Reassuringly, ESI-MS analysis provided a molecular mass of 72 122.2 kDa. This corresponded well with the calculated molecular mass of *Sc*PPDC-His lacking the two N-terminal residues, Met and Ala (72 113.6 kDa). The N-terminal sequence of *Sc*PPDC-His was determined to be PVTIEKFV, corresponding to residues 3–10 of the expected *Sc*PPDC sequence, confirming that the N-terminal Met and Ala were indeed absent. Although cleavage of the terminal Met was not unexpected, the loss of the alanine residue was initially surprising. However, the literature revealed several examples in which the presence of proline as the antepenultimate residue led to the removal of both methionine and alanine. These include interleukin-2 [27] and the bullfrog ribonuclease RNaseRC-4 [28], both expressed in *E. coli*.

Although ThDP-dependent decarboxylases are generally tetrameric [29], gel filtration of native *Sc*PPDC-His revealed that *Sc*PPDC-His exists in solution primarily as a dimer, with a small proportion (< 15%) of tetramer (data not shown). Although unusual, this is not without precedent because recent studies have shown that the branched-chain keto acid decarboxylase (KdcA) from *Lactococcus lactis* is a homodimer both in crystals [30] and solution [31].

The pH optimum of *Sc*PPDC-His was found to be in the range 6.5–7.0, with activity falling sharply above pH 7.0 (Fig. 3). This is typical for a ThDP-dependent enzyme and likely relates to the pK_a of the 4′-aminopyridinium group on the cofactor [32]. As a consequence, unless noted otherwise, kinetic characterizations were carried out at pH 7.0.
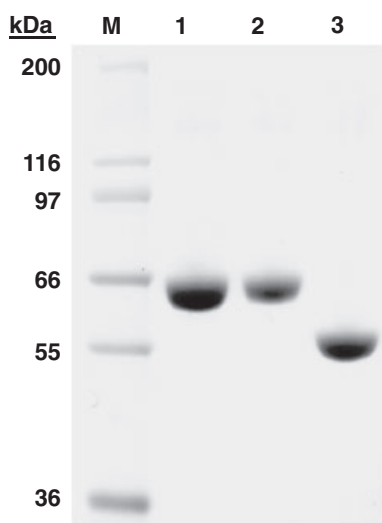
Fig. 2. Purified protein samples were run on a 4–12% Bis-Tris/Mops-SDS gel. Lanes: 1, Mark 12 MW standards (Invitrogen); 2, *Sc*PPDC-His; 3, *Sc*PPDCE545L-His; 4, BFDC-His. BFDC, a typical ThDP-dependent decarboxylase with a molecular mass of approximately 57 kDa, is included for comparison.
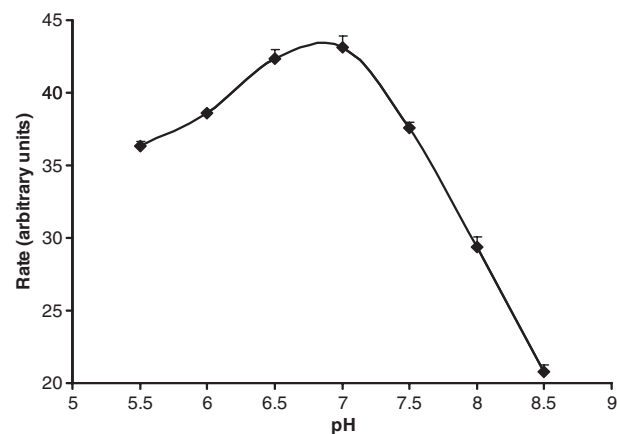
Fig. 3. pH Screen of *Sc*PPDC-His. The pH optimum of *Sc*PPDC-His was determined as described in the Materials and methods. Each point represents the mean ± SEM of three separate determinations.

Although the specific activity of *Sc*PPDC has been measured for several substrates using crude cell extracts [4], to date, there has been no comprehensive examination using the purified enzyme. Accordingly, the kinetic parameters for a selection of 2-keto acids were determined for *Sc*PPDC-His. The 2-keto acids were chosen to provide information on (a) the specificity of the enzyme for the products of amino acid catabolism and (b) the overall substrate specificity of *Sc*PPDC. As shown in Table 1, phenylpyruvic acid (PPA) and indolepyruvic acid (IPyA) were the preferred substrates. On the basis of K_m values, IPyA had higher affinity for the enzyme than PPA, although decarboxylation of the former proceeded more slowly. 4-Hydroxyphenylpyruvate, the substrate derived from tyrosine, had a similar affinity to PPA for *Sc*PPDC-His but was decarboxylated at approximately half the rate.

By comparison, 2-keto acids derived from aliphatic amino acids were much poorer substrates for *Sc*PPDC-His (Table 1). It was notable that much of the reduced activity could be related to substrate binding rather than k_{cat} effects. With the exception of PPA (20 s^{-1}), k_{cat} values for the aromatic substrates were approximately 10 s^{-1}. The methionine-derived substrate, 4-methylthio-2-ketobutanoic acid, bound to the enzyme with approximately 20-fold lower affinity than IPyA but was turned over more quickly, with a k_{cat} value approaching 8 s^{-1}. A similar result was observed for the non-natural substrate, 2-ketohexanoic acid and the branched-chain 2-keto acid derived from leucine, 4-methyl-2-ketopentanoic acid. The k_{cat} value for the isoleucine derivative, 3-methyl-2-ketopentanoic acid, was similar to that of its structural isomer but its K_m

value was approximately three-fold higher, as well as 30-fold higher than that for PPA.

The shorter straight chain 2-keto acids (2-ketopentanoic acid, 2-ketobutanoic acid and pyruvic acid) exhibited K_m values approximately 20- to 100-fold higher than that for PPA, with the values increasing as the chain length decreased. The k_{cat} values for the C4, C5 and C6 2-keto acids also decreased as the chain length decreased but, in general, they were broadly similar to those of the other substrates tested. The combination of a smaller side chain and the presence of a 3-methyl substituent resulted in the biggest decrease in k_{cat}/K_m for a 'natural' substrate. Even then the 80-fold increase in K_m value for the valine derivative, 3-methyl-2-ketobutanoic acid, suggested that the problem was an inability to bind the substrate rather than problems with turnover. It was not until pyruvate that an order of magnitude decrease in k_{cat} value was observed.

As described above, *Sc*PPDC was able to utilize aliphatic 2-keto acids, albeit with reduced efficiency. To further explore effect of chain length on substrate specificity, we looked at the reaction of *Sc*PPDC with benzoylformic acid (2-keto-2-phenylethanoic acid) and 2-keto-4-phenylbutanoic acid. These substrates have a phenyl group attached to a 2C and a 4C keto acid, respectively. Of the two, benzoylformate was the poorer substrate and it was only possible to collect kinetic data under *V/K* conditions. Interestingly, 2-keto-4-phenylbutanoic acid proved to be the first substrate where the effect of an alteration in chain length was primarily manifested in the k_{cat} value. For example, although its K_m value was similar to that of PPA and 4-hydroxyphenylpyruvate, 2-keto-4-phenylbutanoate

Table 1. ScPPDC substrate profile. Mean ± SEM of at least three separate determinations for reactions carried out at pH 7.0. ND, not determined; NAD, no activity detected.

Substrate	Amino acid	K_m (mM)	k_{cat} (s^{-1})	k_{cat}/K_m (mM^{-1}·s^{-1})	%[a]
Phenylpyruvic acid	Phe	0.10 ± 0.01	20 ± 2.1	200	100
Indole-3-pyruvic acid	Trp	0.03 ± 0.01	5.4 ± 0.3	200	100
4-Hydroxyphenylpyruvic acid	Tyr	0.09 ± 0.01	11 ± 0.8	125	63
4-Methylthio-2-ketobutanoic acid	Met	0.64 ± 0.03	7.7 ± 0.1	12	6
4-Methyl-2-ketopentanoic acid	Leu	0.90 ± 0.03	10 ± 0.1	11	6
3-Methyl-2-ketopentanoic acid	Ile	3.1 ± 0.3	11 ± 0.6	3.5	2
3-Methyl-2-ketobutanoic acid	Val	8.5 ± 0.4	19 ± 0.5	2.2	1
2-Keto-4-phenylbutanoic acid		0.09 ± 0.01	1.7 ± 0.01	19	9
2-Ketohexanoic acid		0.69 ± 0.01	8.8 ± 0.1	13	6
2-Ketopentanoic acid		2.1 ± 0.1	5.2 ± 0.1	2.5	1
2-ketobutanoic acid		7.6 ± 0.6	3.9 ± 0.1	0.52	0.2
Pyruvic acid		9.7 ± 0.1	0.34 ± 0.01	0.035	0.02
Benzoylformic acid		ND	ND	0.35[b]	0.2
3-Indoleglyoxylic acid		NAD	–	–	–

[a] Percentage of k_{cat}/K_m for PPA. [b] *V/K* conditions used.

was turned over approximately 14-fold and seven-fold more slowly than PPA and 4-hydroxyphenylpyruvate, respectively. Finally, *Sc*PPDC was unable to utilize 3-indoleglyoxylic acid as a substrate. Thus, the activity of the enzyme with the indole-derived substrates, 3-indoleglyoxylic acid and IPyA, somewhat paralleled that with benzoylformic acid and PPA.

The *ARO10* gene was initially found to be inducible by tryptophan [13] and later by phenylalanine [3], suggesting that *Sc*PPDC is likely to have indole-3-pyruvate and phenylpyruvate decarboxylase activity, respectively. It was also noted that the *ARO10* gene was subject to the same regulatory mechanism as the *ARO9* gene, which encodes aromatic aminotransferase II [13]. The latter is inducible by all the aromatic amino acids and so it is not entirely unexpected that *Sc*PPDC was found to decarboxylate 4-hydroxyphenyl-pyruvate (Table 1).

It has been proposed that a single decarboxylase activity was responsible for the catabolism of leucine, methionine and phenylalanine [4]. Conversely, Dickinson *et al.* [2] reported that *Sc*PPDC contributed only 6% of the isoleucine flux. The results obtained in the present study show that the efficiency of leucine decarboxylation is only 5% of that of phenylalanine, suggesting that Dickinson *et al.* [2] are more likely to be correct. *Sc*PPDC has a relatively low, but measurable, activity with the isoleucine-derived, 3-methyl-2-keto-pentanoic acid. This is also consistent with the report that an *ARO10* (*YDR380w*) knockout was able to grow using isoleucine as sole nitrogen source but that, in the absence of other pyruvate decarboxylases, the presence of the *Sc*PPDC was sufficient to allow cell growth. Perpète *et al.* [9] reported that *Sc*PPDC was essential for the decarboxylation step in methionine catabolism. If it is assumed that, similar to the other amino acids catabolized to fusel alcohols in yeast, methionine was solely catabolized by the Ehrlich pathway, this observation would appear to be at odds with the relatively poor usage of 4-methylthio-2-ketobuta-noic acid (Table 1). However, Perpète *et al.* [9] also demonstrated that Met may be catabolized by trans-amination to 4-methylthio-2-ketobutanoic acid, then demethiolation, yielding methanethiol and 2-ketobuty-rate. Unlike the fusel alcohols, 2-ketobutyrate provides a useful carbon skeleton. Thus, although *S. cerevisiae* may indeed be able to catabolize Met through the Ehrlich pathway via *Sc*PPDC, this route would be less beneficial to the organism which, in turn, is reflected in the relatively low k_{cat}/K_m value for 4-methylthio-2-ketobutanoic acid.

Overall, these data show that substrates derived from the aromatic amino acids are clearly preferred over those from aliphatic amino acids and confirm that *Sc*PPDC, the *ARO10* gene product, is an efficient aromatic 2-keto acid decarboxylase, consistent with its proposed *in vivo* role in phenylalanine and tryptophan catabolism [2]. It may also be involved in tyrosine metabolism but, when alternative pathways are available, it is unlikely to play any significant role in the catabolism of the branched-chain amino acids or of methionine.

Identification and mutation of residues affecting substrate specificity

There are two histidine residues in the active site of *Sc*PDC located adjacent to each other on a single monomer [33]. This effectively forms a 'HH' motif that is conserved in other PDCs [34,35] and PDC-like decarboxylases such as KdcA, the branched-chain keto acid decarboxylase from *L. lactis* [30], the indole-3-pyruvate decarboxylase from *Enterobacter cloacae* (*Ec*IPDC) [36] and the PPDC from *Azospirillum brasi-lense* (*Ab*PPDC) [37]. The last two enzymes are discussed in more detail below.

CLUSTALW alignment of the sequence of *Sc*PPDC with those of *Sc*PDC, *Zm*PDC, KdcA and *Ec*IPDC suggested that Ile335, Gln448 and Met624 were likely to shape its substrate binding pocket. This was confirmed using a homology model (Fig. 4A) of *Sc*PPDC obtained from the PHYRE server (http://www.sbg.bio.i-c.ac.uk/phyre/) using the structure of KdcA [Protein Data Bank (PDB): 2VBG] as the template. It is clear from Fig. 4B, which was obtained by superimposing the cofactors of several 'HH' motif decarboxylases, that the relative size of the substrates is inversely proportional to the size of the residues. Accordingly, three mutants (I335Y, Q464W and M624W) were prepared with a view to enhancing the activity of *Sc*PPDC towards the shorter chain-length substrates such as pyruvate, and the unbranched substrates, which the wild-type enzyme does not favor (Table 1).

The results, provided in Table 2, confirm that all three residues are important for catalysis by *Sc*PPDC. The k_{cat} value for reaction of each variant with PPA is lower than that of the wild-type enzyme and, with the exception of Q448W, K_m values are increased and k_{cat}/K_m values are reduced by almost two orders of magnitude. When viewed as a whole, it is apparent that these mutations have had the most beneficial effect on the decarboxylation of 2-ketopentanoic acid. Each variant has a K_m value less than 1 mM, which is lower than that of the wild-type enzyme, as well as k_{cat}/K_m values that are greater than that of the wild-type enzyme. This trend does not extend to the shorter

Fig. 4. (A) Superposition of the homology model of the ScPPDC dimer (orange) and the template (KdcA, PDB: 2VGB, cyan). The left hand side of the figure shows several of the additional loops necessary to account for the 20% greater molecular mass of the former. (B) Superposition of the putative substrate binding residues of *Sc*PPDC (orange), KdcA (cyan) IPDC (PDB: 1OVM, magenta) and *Zm*PDC (PDB: 2WVA, yellow). The pyruvate and triazole-ThDP (elemental colors) were from PDB: 2WVA. The dots represent the van der Waals radius of the methyl group of pyruvate.
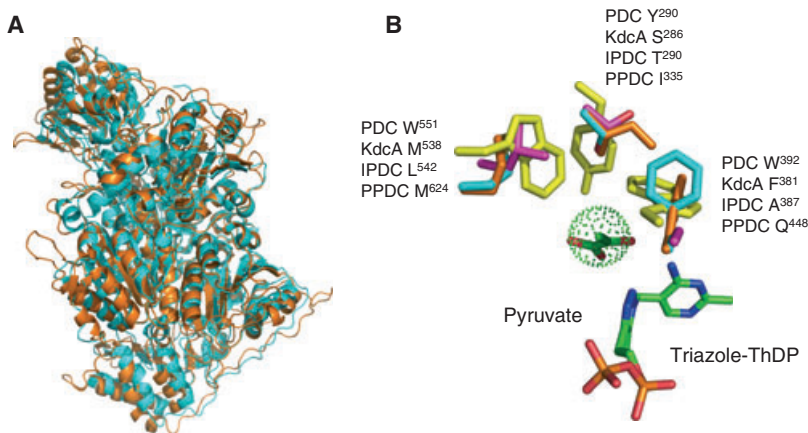
Table 2. Activity of ScPPDC Variants towards short chain and unbranched substrates (mean ± SD of two or three individual determinations). The data were obtained using the standard assay conditions at pH 6.0. ND, not determined (assayed under V∕K conditions). NAD, no activity detected.

	Wild-type	I335Y	Q448W	M624W	I335Y/M624W
Phenylpyruvic acid					
K_m (mM)	0.10 ± 0.01	0.80 ± 0.03	0.054 ± 0.002	0.18 ± 0.04	ND
k_{cat} (s^{-1})	20 ± 2.1	0.85 ± 0.02	4.8 ± 0.04	1.2 ± 0.07	ND
k_{cat}/K_m (mM^{-1}·s^{-1})	200	1.1 (0.6)[a]	89 (45)	6.7 (3.4)	0.030 (0.02)
2-Ketohexanoic acid					
K_m (mM)	0.48 ± 0.2	0.55 ± 0.10	0.46 ± 0.02	0.17 ± 0.02	1.0 ± 0.2
k_{cat} (s^{-1})	8.8 ± 0.6	3.3 ± 0.04	1.3 ± 0.1	0.96 ± 0.03	0.41 ± 0.06
k_{cat}/K_m (mM^{-1}·s^{-1})	18	6.0 (33)	2.8 (16)	5.8 (32)	0.42 (2.3)
2-Ketopentanoic acid					
K_m (mM)	1.7 ± 0.2	0.63 ± 0.04	0.54 ± 0.08	0.37 ± 0.03	0.96 ± 0.06
k_{cat} (s^{-1})	2.8 ± 0.2	2.1 ± 0.1	2.0 ± 0.01	0.76 ± 0.06	0.39 ± 0 05
k_{cat}/K_m (mM^{-1}·s^{-1})	1.6	3.4 (213)	3.7 (231)	2.1 (131)	0.40 (25)
2-Ketobutanoic acid					
K_m (mM)	7.6 ± 0.6	6.4 ± 1.8	7.0 ± 1.1	5.5 ± 0.8	NAD
k_{cat} (s^{-1})	3.9 ± 0.1	0.06 ± 0.01	2.2 ± 0.1	0.04 ± 0.01	NAD
k_{cat}/K_m (mM^{-1}·s^{-1})	0.51	0.009 (1.7)	0.315 (62)	0.007 (1.4)	NAD
Pyruvic acid					
K_m (mM)	5.7 ± 0.1	25 ± 3	5.5 ± 0.2	6.4 ± 0.9	ND
k_{cat} (s^{-1})	0.26 ± 0.00	0.064 ± 0.004	0.32 ± 0.01	0.45 ± 0.03	ND
k_{cat}/K_m (mM^{-1}·s^{-1})	0.046	0.003 (7)	0.06 (130)	0.07 (152)	0.027 (59)

[a] Comparison of k_{cat}/K_m with wild-type *Sc*PPDC-His for the corresponding substrate (expressed as a percentage).

chain 2-keto acids, 2-ketobutanoate and pyruvate, where the kinetic constants are broadly similar for each variant. That said, even the latter observation is in sharp contrast to the results for PPA where the individual variants showed significant decreases in k_{cat}/K_m values. In a previous study, the corresponding variants of the branched-chain decarboxylase from *L. lactis*, KdcA, were prepared [38]. In those cases, an improvement was observed for the binding of pyruvate but, overall, k_{cat}/K_m for pyruvate remained well below those obtained for the natural substrate, 3-methyl-2-ketopentanoic acid.

Attempts were made to prepare the combinations of double mutants, as well as the triple mutant. Of these, only the I335Y/M624W variant was produced as soluble protein. Although the kinetic data for this variant, also provided in Table 2, indicated that PPA was no longer a viable substrate, there was also little improvement in the utilization of aliphatic substrates. The difficulties with the stability of the double and triple mutants mirrored that observed with KdcA [38]. Although a single site mutant of PDC has been shown to possess excellent 2-ketohexanoate decarboxylase activity [15], the results reported in the present study

reinforce those of the KdcA study, which suggest that mutation of single residues is unlikely to produce an 'instant' PDC. It appears that it will be easier to expand the active site to accept larger substrates and, as shown for benzoylformate decarboxylase [16], saturation mutagenesis of at least two residues will be required to shift the substrate preference towards pyruvate. This finding is consistent with the recent study carried out by Steinmetz *et al.* [39] which showed that, in the ThDP-dependent acetohydroxy acid synthase, two residues act in concert to mediate substrate binding and specificity. Concomitantly, both residues orient substrates and intermediates to ensure optimal alignment of orbitals throughout the reaction [39].

Comparison with other aromatic 2-keto acid decarboxylases

To date, there has been only one detailed characterization of a phenylpyruvate decarboxylase, the *pdc* gene product from the nitrogen-fixing bacterium, *A. brasilense*. Initially, this enzyme was identified as an indole-3-pyruvate decarboxylase because it played a central role in the formation of indole acetic acid, the most abundant naturally occurring auxin [40,41]. However, subsequent analysis showed that its substrate spectrum was markedly different to that of the homologous IPDC from *E. cloacae* [19]. For example, in addition to IPyA, the *Ec*IPDC was able to decarboxylate both benzoylformate and pyruvate [42,43], but not PPA [40,42]. Furthermore, there was no evidence for substrate activation of *Ec*IPDC [42]. Conversely, the *A. brasilense* enzyme showed a ten-fold greater k_{cat}/K_m for PPA than for IPyA, no activity with benzoylformate, and substrate activation was observed with IPyA and several other substrates [19]. Ultimately, this led to the classification of the *A. brasilense ipd*C gene product as a phenylpyruvate decarboxylase (*Ab*PPDC).

The data provided in Table 1 indicate that *Sc*PPDC is quite different to both *Ab*PPDC and *Ec*IPDC in that it is able to decarboxylate PPA and IPyA, essentially with equal efficiency. It is more like *Ab*PPDC in that it can also decarboxylate 4-phenyl-2-ketobutanoic acid and 2-ketohexanoic acid, although it does so without evidence for substrate activation. On the other hand, *Sc*PPDC can decarboxylate 3- and 4-methyl-2 ketopentanoic acid, as well as benzoylformate, whereas *Ab*PPDC cannot [19]. In short, the activities of the two phenylpyruvate decarboxylases are similar yet different, and both are distinct from those of *Ec*IPDC.

A multiple sequence alignment of a suite of known and putative bacterial PPDCs and IPDCs showed that the sequences divided into two clades, indicating that

they have derived from at least two different ancestors [19]. The sequences in one clade all possessed a glutamic acid residue at the position corresponding to residue 468 of *Ec*IPDC. In the second clade, which included *Ab*PPDC, in most cases, the glutamate was replaced by a leucine. Consequently, it was speculated that the specificity for IPyA or PPA might be determined by the presence of a glutamic acid or a leucine, respectively, in this position. Expansion of this alignment to include yeast PPDC homologs shows that the yeast sequences cluster with the 'IPDC' group, all having Glu at this position (data not shown). To explore this issue further, the Glu545Leu variant of *Sc*PPDC was prepared, and its kinetic parameters with the two substrates, PPA and IPyA, were determined. A comparison of these and the parameters of the wild-type enzyme are presented in Table 3.

*Sc*PPDC-E545L was unstable in the buffer used for the IPyA assay and thus was assayed in the standard buffer but with the loss of NADH monitored at 366 nm. Unexpectedly, this variant showed evidence of allosteric activation by both PPA and IPyA, with Hill coefficients of 1.8 and 2.1, respectively. By contrast, the wild-type enzyme showed little evidence of allosteric activation with Hill coefficients approaching 1 for both substrates. Comparison of $S_{0.5}$ values showed that both substrates bound with higher affinity to the E545L variant. For PPA, the affinity increased almost 30-fold, although this was accompanied by a decrease in k_{cat} value of more than 700-fold. For IPyA, a three-fold increase in binding affinity was observed, with a concomitant 38-fold decrease in k_{cat} value. Overall, although the *Sc*PPDC-E545L variant is a much poorer decarboxylase than the wild-type enzyme, it could be argued that, with a 15 : 9 ratio of $k_{cat}/S_{0.5}$, the substrate preference has been switched to favor IPyA. Of

Table 3. Activity of E545L *Sc*PPDC-His. All data were obtained at pH 7.0 and were analyzed using the simplified Hill equation.

	Wild-type	E545L[a]
Phenylpyruvic acid		
$S_{0.5}$ (µM)	97 ± 8	3.4 ± 0.3 (29)
k_{cat} (s^{-1})	22 ± 2.1	0.03 ± 0.002 (730)
$k_{cat}/S_{0.5}$ (mM^{-1}·s^{-1})	226	8.8 (25)
n_h	1.06 ± 0.06	1.84 ± 0.14
Indole-3-pyruvic acid		
$S_{0.5}$ (µM)	27 ± 3	9.6 ± 1.7 (2.8)
k_{cat} (s^{-1})	5.3 ± 0.2	0.14 ± 0.01 (38)
$k_{cat}/S_{0.5}$ (mM^{-1}·s^{-1})	196	15 (13)
n_h	1.15 ± 0.13	2.13 ± 0.27

[a] The fold decrease from wild-type enzyme is shown in parentheses.

course, this is the opposite result to that expected if a leucine residue in this position was truly indicative of an enzyme being a PPDC [19].

Although it is possible to argue about whether there is a true switch in substrate preference, the data provided in Table 3 show conclusively that the E545L variant has (a) enhanced affinity for both PPA and IPyA and (b) evidence for allosteric activation that was not present in the wild-type enzyme. What is not clear are the reasons for those observations. *Sc*PPDC Glu545 has well characterized equivalents in *Ec*IPDC (Glu468), *Zm*PDC (Glu473) and *Sc*PDC (Glu477) and forms part of a Glu-Asp-His triad that has long been associated with the various protonation–deprotonation steps in the decarboxylation reaction [43–47]. Early modeling studies suggested that Glu477 (*Sc*PDC) participates in the decarboxylation of the 2-lactyl-thiamin diphosphate intermediate, as well as in the protonation of the carbanion–enamine intermediate [44]. These predictions were recently confirmed experimentally using a combination of CD and NMR spectroscopy using the E473D and E473Q variants of *Zm*PDC [47]. It is interesting to note that these variants both showed an approximately 1000-fold decrease in the value of k_{cat}, similar to that observed for the E477Q variant of *Sc*PDC [46], whereas the E468D variant of *Ec*IPDC showed an approximately 25-fold decrease in the value of k_{cat} [43]. In all cases, the K_m values were essentially unaffected by the mutation [43,46,47]. In our case, the E545L variant showed, depending on the substrate, decreases in k_{cat} reminiscent of both pyruvate and IPyA decarboxylases, although these decreases were accompanied by a concomitant decrease in K_m values for PPA and IPyA (Table 3). Given that replacement of this glutamic acid residue results in relatively large (two or three orders of magnitude) changes in k_{cat} values, it is noteworthy that *Ab*PPDC, which has a leucine at the corresponding position, has a k_{cat} value of 5.6 s^{-1} [19]. This value is broadly similar to the k_{cat} values of *Ec*IPDC (3.9 s^{-1}) [42], *Sc*PDC (36 s^{-1}) [46] and *Sc*PPDC (20 s^{-1}) (Table 1) with their natural substrates. Clearly, *Ab*PPDC has been able to adapt, and it was suggested that this was achieved by Leu462 providing an increase in the hydrophobicity of the active site, thereby stabilizing zwitterionic intermediates [37]. Nevertheless, the catalytic mechanism of a ThDP-dependent decarboxylase requires a number of proton transfer steps, and these are often mediated through a network of water molecules. Removal of a hydrophilic residue such as E545 has the potential to disrupt any hydrogen bonding/water molecule network, which will also result in a reduction in k_{cat} values. It is conceivable that, for the *Sc*PPDC E545L variant, the increase

in hydrophobicity is insufficient to compensate for the loss of an acid–base catalyst, or the disruption of a hydrogen bond network, although it does result in an increase in binding affinity for PPA and IPyA.

One question still remains: why does the E545L variant show allosteric activation? Again, the answer may lie with *Ab*PPDC. It has been proposed that, rather than the typical Glu-Asp-His motif, *Ab*PPDC has an Asp-Asp-His catalytic triad in which Asp282 replaces the glutamic acid residue. Moreover, it is only after the substrate binds at the regulatory site that Asp282 moves into the active site to form the catalytic triad [48]. In Glu334, *Sc*PPDC has a residue occupying a similar position to Asp282 and which, potentially, may act as a surrogate for Glu545 in the catalytic triad (albeit with a reduced effect). The observation of allosteric activation would then arise from a requirement for the substrate to bind to effect the correct positioning of Glu334 for catalysis. Of course, this explanation also requires a second, regulatory, substrate binding site. In *Ab*PPDC, the second phenylpyruvate is held tightly by charged interactions of its carboxylate with two arginine residues (Arg60 andArg215) and a hydrogen bond to the backbone of Ala397, while the phenyl ring forms a cation–π interaction with Arg214 [48]. Intriguingly, superposition of the *Sc*PPDC model and the *Ab*PPDC-3dThDP-PPA (PDB: 2Q5O) indicates that a similar site may be present in the former. In Arg88 and Arg267, *Sc*PPDC has positional counterparts for Arg60 and Arg215, respectively. The amide of Ser464 is similarly located to that of Ala397in *Ab*PPDC and, although *Sc*PPDC has no direct counterpart to Arg214, there is a lysine residue, Lys461, that could rotate in and perform a similar function to Arg214. Clearly, this explanation is speculative, although it does provide a basis for our ongoing investigations. As an aside, previous results reported by Meyer *et al.* [47] also suggest that the enamine of the E545L variant is likely to be long lived, raising the possibility that this variant may carry out more efficient carboligation reactions than the wild-type enzyme. This too is being explored in our continuing studies.

In summary, we have demonstrated that the *S. cerevisiae ARO10* gene product comprises an efficient phenylpyruvate decarboxylase likely playing a prominent role in the catabolism of aromatic, but not aliphatic, amino acids. Furthermore, we have reinforced previous studies concluding that it will take more than point mutations to significantly alter substrate specificity in ThDP-dependent decarboxylases. Finally, we have that shown that it is unlikely that replacement of a glutamic acid by leucine leads to discrimination between the two substrates, phenylpyruvate and

indolepyruvate, although it did lead to unexpected allosteric activation.

Materials and methods

Reagents

S. cerevisiae genomic DNA was obtained from Novagen (EMD4Biosciences, Gibbstown, NJ, USA). PCR primers were purchased from Integrated DNA Technologies (Coralville, IA, USA). The sequences of the primers are provided in Table S1. Nickel-nitrilotriacetic acid resin was obtained from Qiagen (Valencia, CA, USA). Substrates were purchased from Sigma–Aldrich (St Louis, MO, USA), Acros (Morris Plains, NJ, USA) and ChemBridge (San Diego, CA, USA). Buffer and assay components were from Sigma–Aldrich or Fisher Scientific (Pittsburgh, PA, USA) and were of the highest commercially-available quality.

Amplification

The coding region for *Sc*PPDC (*ARO10*) was amplified *S. cerevisiae* genomic DNA using the primer pair PPDC-NdeI and PPDC-XhoI, which inserted *Nde*I and *Xho*I sites at the 5′ and 3′ ends, respectively, of the *Sc*PPDC gene. The amplified fragment was gel-purified then ligated into pCRBlunt (Invitrogen, Carlsbad, CA, USA) and the resulting plasmid transformed into chemically-competent *E. coli* TOP10 cells. Plasmid DNA from the transformants was purified and the *Nde*I-*Xho*I fragment inserted into a modified pET17b vector (Novagen) to give the expression vector, pET17PPDC-His, thereby permitting Ni-chelate affinity purification of *Sc*PPDC-His. The fidelity of the amplification and vector construction was confirmed by sequencing of pET17PPDC-His (University of Michigan DNA Sequencing Core Facility, Ann Arbor, MI, USA).

Mutagenesis

Single residue variants of *Sc*PPDC-His were prepared by the QuikChange method (Stratagene, Agilent Technologies Inc., Santa Clara, CA, USA) using pET17PPDC-His and the primers listed in Table S1. The presence of the changed nucleotides was screened by restriction digestion and confirmed by sequencing.

Purification

*Sc*PPDC-His and its variants were overexpressed in *E. coli* BL21(DE3)pLysS cells (Novagen). *Sc*PPDC-His expression was induced at room temperature with isopropyl thio-β-D-galactoside and the cultures grown for 20 h. All subsequent *Sc*PPDC-His purification procedures were performed at 4 °C. Cells were pelleted by centrifugation and resuspended in buffer A (50 mM NaPO$_4$, pH 8.0, 300 mM NaCl) containing 5 mM imidazole, then frozen at −80 °C overnight. The frozen cells were thawed and incubated for 30 min with DNase (5 µg·mL^{-1}) and lysozyme (0.2 mg·mL^{-1}) then disrupted by sonication (3 × 30 s bursts, with 1 min rest between bursts). Clarified cell-free extract was obtained by two centrifugation steps of 30 min at 20 000 *g*.

The cell-free extract was applied to a nickel-nitrilotriacetic acid (Qiagen) column attached to a Biologic LC system (Bio-Rad, Hercules, CA, USA) and equilibrated with buffer A. The column was extensively washed with buffer A and weakly-bound proteins eluted with buffer B (buffer A containing 20 mM imidazole). *Sc*PPDC-His was eluted with buffer C (buffer A containing 250 mM imidazole). Fractions containing *Sc*PPDC-His were pooled, then desalted and exchanged into storage buffer (50 mM KPO$_4$, pH 7.0, 1 mM MgSO$_4$, 0.5 mM ThDP, 10% glycerol) using an Econo-Pac DG10 desalting column (Bio-Rad). The purified protein was concentrated (Amicon Ultra, Millipore, Billerica, MA, USA) and stored at −80 °C.

The purity of the *Sc*PPDC-His was verified by SDS/PAGE. The protein concentration was determined spectrophotometrically using $\varepsilon_{280} = 71260$ M^{-1}·cm^{-1} calculated with PROT PARAM (http://expasy.org/tools/protparam.html) or by the Bradford assay using BSA as standard.

Assay

The decarboxylation activity of *Sc*PPDC-His on a range of aromatic and aliphatic 2-keto acids was monitored at 30 °C by a coupled assay described previously [38]. The reaction mixture contained (in 1 mL): 100 mM KPO$_4$ buffer (pH 6.0 or 7.0); 1 mM MgSO$_4$; 0.5 mM ThDP; 200 µM NADH; 0.05–0.25 U horse liver alcohol dehydrogenase or yeast alcohol dehydrogenase and varying concentrations of 2-keto acid. The reaction was initiated by addition of *Sc*PPDC-His (2.5–190 µg·mL^{-1}) and the loss of NADH was monitored at 340 nm. Stock solutions of the 2-keto acids were usually prepared in assay buffer (100 mM KPO$_4$, 1 mM MgSO$_4$, 0.5 mM ThDP) and the pH adjusted to 6.0 or 7.0 as required. When necessary, *Sc*PPDC-His was diluted into assay buffer containing 1 mg·mL^{-1} BSA.

Monitoring the decarboxylation of IPyA had been reported by Schütz *et al.* [42] to be problematic. Consequently, IPyA decarboxylation by *Sc*PPDC was determined in an assay buffer containing 10 mM Mes buffer (pH 6.5), 1 mM MgSO$_4$ and 0.5 mM ThDP, with the reaction being monitored at 366 nm to reduce interference as a result of the high absorbance of IPyA at 340 nm [19]. IPyA stock solutions were prepared in assay buffer and incubated for 45–60 min at room temperature to ensure maximal conversion from the enol to the keto tautomer [42]. The E545L variant precipitated in this buffer and therefore was assayed under the standard conditions used for all other substrates, although the reaction was monitored at 366 nm.

Analysis of enzyme kinetics data was performed with the ENZYME KINETICS package within SIGMAPLOT (Systat Software, Inc., Chicago, IL, USA), using the single-substrate model and Michaelis–Menten and Hill analysis.

The pH optimum of *Sc*PPDC-His for the decarboxylation of PPA was determined by the coupled assay described above, using a *Sc*PPDC-His concentration of 2.5 µg·mL^{-1} and PPA at 0.62 mM. The pH determined in this screen was used for all subsequent experiments unless otherwise stated.

Size-exclusion chromatography

The molecular mass of native *Sc*PPDC-His was determined by size exclusion chromatography on a Sephacryl S-200 HR Column (1.6 × 94 cm), equilibrated with 50 mM NaPO$_4$, 150 mM NaCl (pH 7.0). The void volume of the column was determined with Blue Dextran, and the elution volume of *Sc*PPDC-His compared with those of ferritin (440 kDa), aldolase (158 kDa), conalbumin (75 kDa) and albumin (43 kDa) (GE Healthcare HMW Gel Filtration Standards; GE Healthcare, Milwaukee, WI, USA). In addition, *P. putida* BFDC was included as a standard because its native molecular mass and multimeric form is well-established [17].

MS and N-terminal sequencing

*Sc*PPDC-His was exchanged into 50 mM Mops, 1 mM MgSO$_4$, 0.5 mM ThDP (pH 7.0) for analysis by LC-MS. N-terminal sequencing was performed following electrophoretic transfer of *Sc*PPDC-His to a poly(vinylidene difluoride) membrane. Both were performed at the University of Michigan Protein Structure Facility (Ann Arbor, MI, USA).

Acknowledgements

References

1 Hazelwood LA, Daran JM, van Maris AJ, Pronk JT & Dickinson JR (2008) The Ehrlich pathway for fusel alcohol production: a century of research on *Saccharomyces cerevisiae* metabolism. *Appl Environ Microbiol* **74**, 2259–2266.

2 Dickinson JR, Salgado LE & Hewlins MJ (2003) The catabolism of amino acids to long chain and complex alcohols in *Saccharomyces cerevisiae*. *J Biol Chem* **278**, 8028–8034.

3 Vuralhan Z, Morais MA, Tai SL, Piper MD & Pronk JT (2003) Identification and characterization of phenylpyruvate decarboxylase genes in *Saccharomyces cerevisiae*. *Appl Environ Microbiol* **69**, 4534–4541.

4 Vuralhan Z, Luttik MA, Tai SL, Boer VM, Morais MA, Schipper D, Almering MJ, Kotter P, Dickinson JR, Daran JM *et al.* (2005) Physiological characterization of the ARO10-dependent, broad-substrate-specificity 2-oxo acid decarboxylase activity of *Saccharomyces cerevisiae*. *Appl Environ Microbiol* **71**, 3276–3284.

5 Atsumi S, Hanai T & Liao JC (2008) Non-fermentative pathways for synthesis of branched-chain higher alcohols as biofuels. *Nature* **451**, 86–89.

6 Zhang K, Sawaya MR, Eisenberg DS & Liao JC (2008) Expanding metabolism for biosynthesis of nonnatural alcohols. *Proc Natl Acad Sci USA* **105**, 20653–20658.

7 Dickinson JR, Lanterman MM, Danner DJ, Pearson BM, Sanz P, Harrison SJ & Hewlins MJ (1997) A ^{13}C nuclear magnetic resonance investigation of the metabolism of leucine to isoamyl alcohol in *Saccharomyces cerevisiae*. *J Biol Chem* **272**, 26871–26878.

8 ter Schure EG, Flikweert MT, van Dijken JP, Pronk JT & Verrips CT (1998) Pyruvate decarboxylase catalyzes decarboxylation of branched-chain 2-oxo acids but is not essential for fusel alcohol production by *Saccharomyces cerevisiae*. *Appl Environ Microbiol* **64**, 1303–1307.

9 Perpete P, Duthoit O, De Maeyer S, Imray L, Lawton AI, Stavropoulos KE, Gitonga VW, Hewlins MJ & Dickinson JR (2006) Methionine catabolism in *Saccharomyces cerevisiae*. *FEMS Yeast Res* **6**, 48–56.

10 Kellermann E, Seeboth PG & Hollenberg CP (1986) Analysis of the primary structure and promoter function of a pyruvate decarboxylase gene (PDC1) from *Saccharomyces cerevisiae*. *Nucleic Acids Res* **14**, 8963–8977.

11 Seeboth PG, Bohnsack K & Hollenberg CP (1990) pdc1(0) mutants of *Saccharomyces cerevisiae* give evidence for an additional structural PDC gene: cloning of PDC5, a gene homologous to PDC1. *J Bacteriol* **172**, 678–685.

12 Hohmann S (1991) Characterization of PDC6, a third structural gene for pyruvate decarboxylase in *Saccharomyces cerevisiae*. *J Bacteriol* **173**, 7963–7969.

13 Iraqui I, Vissers S, Andre B & Urrestarazu A (1999) Transcriptional induction by aromatic amino acids in *Saccharomyces cerevisiae*. *Mol Cell Biol* **19**, 3360–3371.

14 Godard P, Urrestarazu A, Vissers S, Kontos K, Bontempi G, van Helden J & Andre B (2007) Effect of 21 different nitrogen sources on global gene expression in the yeast *Saccharomyces cerevisiae*. *Mol Cell Biol* **27**, 3065–3086.

15 Siegert P, McLeish MJ, Baumann M, Iding H, Kneen MM, Kenyon GL & Pohl M (2005) Exchanging the substrate specificities of pyruvate decarboxylase from *Zymomonas mobilis* and benzoylformate decarboxylase

from *Pseudomonas putida*. *Protein Eng Des Sel* **18**, 345–357.

16 Yep A & McLeish MJ (2009) Evolution of a benzoyl-formate decarboxylase variant with enhanced pyruvate decarboxylase activity. *Biochemistry* **48**, 8387–8395.

17 Hasson MS, Muscate A, McLeish MJ, Polovnikova LS, Gerlt JA, Kenyon GL, Petsko GA & Ringe D (1998) The crystal structure of benzoylformate decarboxylase at 1.6 Å resolution: diversity of catalytic residues in thiamin diphosphate-dependent enzymes. *Biochemistry* **37**, 9918–9930.

18 Ward OP & Singh A (2005) Enzyme biotransformation involving α-ketoacid decarboxylases. In *Microorganisms for Industrial Enzymes and Biocontrol* (Mellado E & Barredo J-L eds), pp. 83–94. Research Signpost, Trivandrum, India.

19 Spaepen S, Versees W, Gocke D, Pohl M, Steyaert J & Vanderleyden J (2007) Characterization of phenylpyruvate decarboxylase, involved in auxin production of *Azospirillum brasilense*. *J Bacteriol* **189**, 7626–7633.

20 Asakawa T, Wada H & Yamano T (1968) Enzymatic conversion of phenylpyruvate to phenylacetate. *Biochim Biophys Acta* **170**, 375–391.

21 Barrowman MM & Fewson CA (1985) Phenylglyoxylate decarboxylase and phenylpyruvate decarboxylase from *Acinetobacter calcoaceticus*. *Curr Microbiol* **12**, 235–240.

22 Guo ZZ (1999) Asymmetric acyloin condensation catalyzed by phenylpyruvate decarboxylase. *Tetrahedron Asymmetry* **10**, 4667.

23 de Boer L, Harder W & Dijkhuizen L (1988) Phenylalanine and tyrosine metabolism in the facultative methyltroph *Nocardia* sp. 239. *Arch Microbiol* **149**, 459–465.

24 Schneider S, Mohamed ME & Fuchs G (1997) Anaerobic metabolism of L-phenylalanine via benzoyl-CoA in the denitrifying bacterium *Thauera aromatica*. *Arch Microbiol* **168**, 310–320.

25 Kishore G, Sugumaran M & Vaidyanathan CS (1976) Metabolism of DL-(+ /–)-phenylalanine by *Aspergillus niger*. *J Bacteriol* **128**, 182–191.

26 Altschul SF, Madden TL, Schaffer AA, Zhang J, Zhang Z, Miller W & Lipman DJ (1997) Gapped BLAST and PSI-BLAST: a new generation of protein database search programs. *Nucleic Acids Res* **25**, 3389–3402.

27 Ben-Bassat A, Bauer K, Chang SY, Myambo K, Boosman A & Chang S (1987) Processing of the initiation methionine from proteins: properties of the *Escherichia coli* methionine aminopeptidase and its gene structure. *J Bacteriol* **169**, 751–757.

28 Liao YD, Jeng JC, Wang CF, Wang SC & Chang ST (2004) Removal of N-terminal methionine from recombinant proteins by engineered *E. coli* methionine aminopeptidase. *Protein Sci* **13**, 1802–1810.

29 Duggleby RG (2006) Domain relationships in thiamine diphosphate-dependent enzymes. *Acc Chem Res* **39**, 550–557.

30 Berthold CL, Gocke D, Wood MD, Leeper FJ, Pohl M & Schneider G (2007) Structure of the branched-chain keto acid decarboxylase (KdcA) from *Lactococcus lactis* provides insights into the structural basis for the chemoselective and enantioselective carboligation reaction. *Acta Crystallogr D Biol Crystallogr* **63**, 1217–1224.

31 Gocke D, Nguyen CL, Pohl M, Stillger T, Walter L & Muller M (2007) Branched-chain keto acid decarboxylase from *Lactococcus lactis* (KdcA), a valuable thiamine diphosphate-dependent enzyme for assymmetric C-C bond formation. *Adv Synth Catal* **349**, 1425–1435.

32 Nemeria N, Korotchkina L, McLeish MJ, Kenyon GL, Patel MS & Jordan F (2007) Elucidation of the chemistry of enzyme-bound thiamin diphosphate prior to substrate binding: defining internal equilibria among tautomeric and ionization states. *Biochemistry* **46**, 10739–10744.

33 Arjunan P, Umland T, Dyda F, Swaminathan S, Furey W, Sax M, Farrenkopf B, Gao Y, Zhang D & Jordan F (1996) Crystal structure of the thiamin diphosphate-dependent enzyme pyruvate decarboxylase from the yeast *Saccharomyces cerevisiae* at 2.3 Å resolution. *J Mol Biol* **256**, 590–600.

34 Dobritzsch D, Konig S, Schneider G & Lu G (1998) High resolution crystal structure of pyruvate decarboxylase from *Zymomonas mobilis*. Implications for substrate activation in pyruvate decarboxylases. *J Biol Chem* **273**, 20196–20204.

35 Kutter S, Wille G, Relle S, Weiss MS, Hubner G & Konig S (2006) The crystal structure of pyruvate decarboxylase from *Kluyveromyces lactis*. Implications for the substrate activation mechanism of this enzyme. *FEBS J* **273**, 4199–4209.

36 Schutz A, Sandalova T, Ricagno S, Hubner G, Konig S & Schneider G (2003) Crystal structure of thiamindiphosphate-dependent indolepyruvate decarboxylase from *Enterobacter cloacae*, an enzyme involved in the biosynthesis of the plant hormone indole-3-acetic acid. *Eur J Biochem* **270**, 2312–2321.

37 Versées W, Spaepen S, Vanderleyden J & Steyaert J (2007) The crystal structure of phenylpyruvate decarboxylase from *Azospirillum brasilense* at 1.5 A resolution. Implications for its catalytic and regulatory mechanism. *FEBS J* **274**, 2363–2375.

38 Yep A, Kenyon GL & McLeish MJ (2006) Determinants of substrate specificity in KdcA, a thiamin diphosphate-dependent decarboxylase. *Bioorg Chem* **34**, 325–336.

39 Steinmetz A, Vyazmensky M, Meyer D, Barak ZE, Golbik R, Chipman DM & Tittmann K (2010) Valine 375 and phenylalanine 109 confer affinity and specificity for pyruvate as donor substrate in acetohydroxy acid

synthase isozyme II from *Escherichia coli*. *Biochemistry* **49**, 5188–5199.

40 Koga J, Adachi T & Hidaka H (1992) Purification and characterization of indolepyruvate decarboxylase. A novel enzyme for indole-3-acetic acid biosynthesis in Enterobacter cloacae. *J Biol Chem* **267**, 15823–15828.

41 Costacurta A, Keijers V & Vanderleyden J (1994) Molecular cloning and sequence analysis of an *Azospirillum brasilense* indole-3-pyruvate decarboxylase gene. *Mol Gen Genet* **243**, 463–472.

42 Schutz A, Golbik R, Tittmann K, Svergun DI, Koch MH, Hubner G & Konig S (2003) Studies on structure-function relationships of indolepyruvate decarboxylase from *Enterobacter cloacae*, a key enzyme of the indole acetic acid pathway. *Eur J Biochem* **270**, 2322–2331.

43 Schutz A, Golbik R, Konig S, Hubner G & Tittmann K (2005) Intermediates and transition states in thiamin diphosphate-dependent decarboxylases. A kinetic and NMR study on wild-type indolepyruvate decarboxylase and variants using indolepyruvate, benzoylformate, and pyruvate as substrates. *Biochemistry* **44**, 6164–6179.

44 Lobell M & Crout DHG (1996) Pyruvate decarboxylase: a molecular modeling study of pyruvate decarboxylation and acyloin formation. *J Am Chem Soc* **118**, 1867–1873.

45 Chang AK, Nixon PF & Duggleby RG (1999) Aspartate-27 and glutamate-473 are involved in catalysis by *Zymomonas mobilis* pyruvate decarboxylase. *Biochem J* **339**, 255–260.

46 Liu M, Sergienko EA, Guo F, Wang J, Tittmann K, Hubner G, Furey W & Jordan F (2001) Catalytic acid-base groups in yeast pyruvate decarboxylase. 1. Site-directed mutagenesis and steady-state kinetic studies on the enzyme with the D28A, H114F, H115F, and E477Q substitutions. *Biochemistry* **40**, 7355–7368.

47 Meyer D, Neumann P, Parthier C, Friedemann R, Nemeria N, Jordan F & Tittmann K (2010) Double duty for a conserved glutamate in pyruvate decarboxylase: evidence of the participation in stereoelectronically controlled decarboxylation and in protonation of the nascent carbanion/enamine intermediate. *Biochemistry* **49**, 8197–8212.

48 Versées W, Spaepen S, Wood MD, Leeper FJ, Vanderleyden J & Steyaert J (2007) Molecular mechanism of allosteric substrate activation in a thiamine diphosphate-dependent decarboxylase. *J Biol Chem* **282**, 35269–35278.

Supporting information

The following supplementary material is available:
Table S1. *Sc*PPDC-His PCR primers.
This supplementary material can be found in the online version of this article.

Please note: As a service to our authors and readers, this journal provides supporting information supplied by the authors. Such materials are peer-reviewed and may be re-organized for online delivery, but are not copy-edited or typeset. Technical support issues arising from supporting information (other than missing files) should be addressed to the authors.